Sustainable Energy & Fuels

ROYAL SOCIETY OF CHEMISTRY

PAPER

View Article Online
View Journal | View Issue

Cite this: *Sustainable Energy Fuels*, 2026, **10**, 1959

Co-pyrolysis of rice straw and empty fruit bunch: effects of blending on product yields and bio-oil composition

Mahendra Tiwari, [a] Meheretu Jaleta Dirbeba, *[b] Alessandro Ruozzi,[b] Juho Lehmusto,[b] Patrik Yrjas[b] and Ravikrishnan Vinu *[a]

Co-processing of agricultural residues is a promising route for producing renewable fuels and chemicals, particularly when feedstock availability is seasonal and material properties vary significantly. In this study, co-pyrolysis of rice straw (RS) and empty fruit bunch (EFB) was investigated using three reactor systems: analytical Py-GC/MS, a single-particle reactor (SPR), and a fluidized-bed reactor (FBR). The two biomasses differ substantially in chemical composition, strongly influencing their pyrolysis behavior. Pyrolysis experiments were conducted at 500 °C for the individual samples and for three blends containing 25%, 50%, and 75% RS (dry weight basis), with the remainder consisting of EFB. RS produced lower bio-oil and higher biochar yields than EFB, primarily due to its higher ash content, particularly alkali and alkaline-earth metals. Higher apparent condensable yields were obtained in the SPR than in the FBR, since the condensable yields in the SPR were estimated by difference. Nonetheless, similar non-condensable gas yields, mainly CO and CO_2, were produced in both reactors. Py-GC/MS analyses showed that the condensable pyrolysis vapors primarily consisted of linear and cyclic oxygenates and phenolic compounds. GC-MS analyses of the bio-oils produced in the FBR revealed a similar composition. RS-derived pyrolysis vapors/bio-oils contained a higher proportion of oxygenates, while the phenolic compounds were more prominent in the EFB vapors/bio-oils. The co-pyrolysis yields closely followed the mixture rule, indicating largely independent decomposition behavior of the RS and EFB in the blend. The results of this study suggest that co-pyrolysis of biomass residues with varying availability and chemical compositions may enhance certain aspects of the fast pyrolysis process and support its overall sustainability.

Received 4th December 2025
Accepted 10th March 2026

DOI: 10.1039/d5se01603g

rsc.li/sustainable-energy

1. Introduction

Renewable energy has become increasingly vital in addressing global environmental challenges and ensuring the security of energy supply. Among renewable energy sources, biomass holds a distinctive position as the only resource capable of providing a renewable supply of fixed carbon.[1] This fixed carbon is indispensable for the production of various fuels and consumer goods, making biomass a crucial component of sustainable energy strategies. Consequently, biomass is a key element of sustainable energy strategies and has the greatest potential among sustainable energy sources to satisfy the energy requirements of modern society.[2] This is particularly important for both developed and developing economies that seek to transition away from fossil fuels. The versatility of biomass is evident in its wide range of sources, including wood, dedicated energy crops, agricultural residues, and forestry waste, all of which can be transformed into energy or valuable chemicals through various thermochemical and biochemical processes.[3–5]

Rice straw (RS) and oil palm empty fruit bunch (EFB) are the most common agricultural residues generated in Asia, having significant potential for the production of important chemicals and fuels. RS, a byproduct of rice cultivation, contributes to over 826 million tonnes (Mt) globally, of which 226 Mt is generated in India every year,[6] while EFB accounts for approximately 22.42 Mt annually in Malaysia alone.[7] RS, rich in cellulose and lignin, is commonly produced in rice-farming regions, while EFB, a byproduct of the palm oil industry, contains high amounts of volatile matter. From the practical implications of feedstock availability, RS is produced in significantly larger quantities and is more widely distributed than EFB, which is geographically limited to palm-oil-producing regions. Therefore, this study evaluates co-pyrolysis primarily in the context of RS-dominated feedstocks, assessing whether the addition of EFB enhances bio-oil yield relative to RS alone under industrially relevant conditions. Thermochemical processes, especially pyrolysis and

[a]*Department of Chemical Engineering, Indian Institute of Technology Madras, Chennai, India. E-mail: vinu@iitm.ac.in; Tel: +91 44 2257 4187*

[b]*High-Temperature Processes and Materials, Faculty of Science and Engineering, Åbo Akademi University, Turku, Finland. E-mail: meheretu.dirbeba@abo.fi; Tel: +358 402 149 444*

gasification, convert biomass into bio-oils and syngas, whereas biochemical methods, such as anaerobic digestion and fermentation, yield biogas and bioethanol. These processes are not only capable of producing renewable fuels but also contribute to reducing greenhouse gas emissions and promoting carbon sequestration.[8] Importantly, biomass energy systems often operate in a closed carbon cycle, where the CO_2 released during thermochemical conversion is offset by CO_2 absorbed during plant growth, making it a carbon-neutral or even carbon-negative option when integrated with technologies, such as carbon capture and storage (CCS).[9] Among the thermochemical processes, pyrolysis is particularly effective in converting biomass into valuable products, *i.e.*, bio-oil and biochar, by heating it in the absence of oxygen.[10] Its flexibility with diverse feedstocks, such as agricultural and forestry residues, makes it suitable for decentralized energy production. The bio-oil from the pyrolysis process can be refined into fuels or chemicals, while the byproduct, pyrolysis off-gases, can be used for electricity or hydrogen production.[11,12] The biochar acts as a long-term carbon sink, improving soil fertility and contributing to carbon sequestration.[13]

Bio-oil derived from conventional fast pyrolysis of lignocellulosic biomass is widely recognized as a promising renewable energy carrier; however, its practical utilization is constrained by its high oxygen content, elevated acidity, chemical instability, and low heating value. These limitations are particularly evident for agricultural residues, which contain high proportions of oxygenated compounds and inorganic constituents that influence pyrolysis pathways. Several studies (*e.g.*, ref. 14 and 15) show that catalytic pyrolysis offers an effective route to address these challenges by facilitating *in situ* deoxygenation, cracking of heavy oxygenated species, and selective upgrading of vapor-phase products. Acidic catalysts, metal oxides, and zeolitic materials have been shown to reduce oxygen-rich compounds, suppress the formation of organic acids, and enhance the yield of aromatics and hydrocarbon-like species.[16] As a result, catalytic fast pyrolysis produces bio-oils with improved chemical stability, reduced acidity, and higher energy density, thereby enhancing their suitability for downstream applications in fuels and chemicals.

Co-pyrolysis or pyrolysis of blends of different biomasses has been reported as another effective method for converting biomass into energy and valuable products, thereby enhancing the yield and quality of the resulting pyrolysis oil compared to pyrolysis of individual feedstocks.[17] Co-pyrolysis can improve the calorific value and reduce the oxygen content of the bio-oil, making it a more viable method for renewable fuel production. Studies indicate that the optimal proportions of mixing biomass feedstocks can significantly influence the biochar, bio-oil, and off-gas yields, with increased pyrolysis temperatures generally enhancing the liquid yield until a maximum is reached.[18] Also, the co-pyrolysis process has the potential to effectively address biomass waste management issues while fostering sustainable energy solutions, reducing dependence on fossil fuels, and mitigating environmental pollution. Pyrolysis of biomass blends provides a practical and sustainable pathway for producing bio-oil and biochar, particularly in India, where feedstock availability is strongly influenced by seasonal harvesting cycles; however, residues such as rice straw, are generated in significant quantities during specific periods and can be efficiently collected and stored for year-round utilization, whereas EFB are typically available in comparatively lower quantities. The storability of such residues enables biomass-based energy systems, including co-pyrolysis processes, to operate in a dispatchable manner, with fuel supplied according to demand. This characteristic fundamentally distinguishes biomass from inherently intermittent renewable resources such as wind energy, which rely on real-time environmental conditions and cannot be stored prior to conversion.[19]

While numerous studies have explored the kinetics of pyrolysis of biomass blends[20–23] and co-pyrolysis of biomass and plastic wastes,[10,24,25] there is a noticeable gap in the pyrolysis of lignocellulosic biomass blends to evaluate pyrolysis product yield and quality, particularly from agro-residues of varying compositions and physical and chemical properties. Co-pyrolysis of these feedstocks could yield synergistic effects, in which interactions among the intermediates generated from the feedstocks enhance the overall economy and sustainability of the pyrolysis process. Ceron *et al.*[22] reported that co-pyrolysis of woody biomass with oil shale decreases the solid residues by 34.4% while improving the process efficiency. Co-pyrolysis of biomass wastes with aquatic plants shows that the process has a positive effect on oil quality and process efficiency.[26] Understanding the interactions between diverse biomass feedstocks during co-pyrolysis could provide valuable insights into optimizing product yields and improving process efficiency.

To the best of the authors' knowledge, this is the first study to systematically investigate the co-pyrolysis of rice straw (RS) and empty fruit bunch (EFB) in fast pyrolysis systems with markedly different heating rates and residence times. By employing three complementary reactors, Py-GC/MS for detailed product characterization, a single particle reactor (SPR) for precise control of pyrolysis conditions, and a fluidized bed reactor (FBR) for scalable bio-oil production, this work provides a comprehensive understanding of feedstock interactions and their influence on pyrolysis product yield and composition. The study offers new insights into the effects of biomass blending on pyrolysis product yields and distribution, advancing efficient and sustainable bioenergy production from diverse agricultural residues.

2. Experimental section

2.1. Preparation of biomass blends

The RS was provided by Sukhbir Agro Energy Limited, Punjab, India, while the EFB was supplied by Valmet Technologies Pvt. Ltd., Chennai, India. The biomass samples were initially cut into smaller pieces (50 mm particle size) using a chaff cutter and dried in an oven at 105 °C for 24 h. To assess the effect of mixing on pyrolysis product yields and distribution, stock blend samples were prepared as follows. The dried RS and EFB samples were mixed in three different weight ratios- 25 : 75, 50 : 50, and 75 : 25 and manually homogenized. For simplicity, these blends are referred to as 25RS, 50RS, and 75RS, respectively. The

mixed samples were subsequently milled to a particle size of <1 mm using a FRITSCH cutting mill (Germany). This additional milling step ensured thorough homogenization and produced a uniform blend. All the experiments involving the blend samples (Sections 2.3–2.5) were conducted using samples taken from these prepared stock blends.

For comparison, pyrolysis experiments were also performed on the individual feedstocks. For this purpose, the dried 50 mm RS and EFB samples were further milled separately to a particle size of <1 mm using the same cutting mill. These milled individual RS and EFB samples were also used for the chemical analyses described in Section 2.2.

2.2. Chemical composition of the biomass feedstocks

Detailed descriptions of the chemical characterization of the RS and EFB samples were reported in our previous study,[6] and the results are provided in Table 1, Section 3.1. These include proximate and ultimate analyses using TGA, Flash 2000 CHNS(O) organic elemental analyzer, ICP-OES; biochemical composition analyses (cellulose, hemicellulose, and lignin), and heating value determinations.

The thermal decomposition behavior of the samples and their blends under pyrolysis conditions was assessed using a thermogravimetric analyzer (TGA; SDT-Q600, TA Instruments). For the TGA analysis, about 3–5 mg of each sample was first weighed into an alumina crucible and placed in the TGA furnace, which was purged with nitrogen at 100 mL min^{-1}. The samples were then heated at 10 °C min^{-1} to 900 °C and held isothermally at this temperature until no further mass loss was observed.

A detailed biochemical characterization of RS and EFB is also provided in our previous study.[6] In that study, glucose was used as an indicator of cellulose-derived sugars and xylose as an indicator of hemicellulose-derived sugars. Since hemicellulose is a heterogeneous polymer composed of multiple monosaccharides, the reported values in our previous study[6] and reproduced in this work (Section 3.1) represent xylose-derived(xylan) fractions rather than total hemicellulose content. Structural carbohydrates were quantified using two-step sulfuric acid hydrolysis followed by HPLC analysis, a widely accepted and literature-consistent method suitable for interpreting pyrolysis behavior. Additional gravimetric holocellulose/cellulose measurements had not been conducted, as doing so would have substantially increased experimental complexity without materially influencing the conclusions of the study.

2.3. Analytical pyrolysis-gas chromatography/mass spectrometry experiments

Pyrolysis of the RS, EFB, and their three mixtures was conducted using a single-shot micro-pyrolyzer (Frontier Lab, PY-3030S) coupled with a gas chromatography-mass spectrometry (GC/MS) system (Shimadzu QP2010 Plus) at 500 °C. The pyrolysis temperature of 500 °C was selected based on its widely reported optimal performance for maximizing bio-oil yields.[27,28] Our previous study[6] also shows maximum condensables yields at 500 °C for the RS and EFB used in this work. At this temperature, devolatilization and primary pyrolysis reactions are largely complete, while higher temperatures provide marginal changes in product distribution with increased energy demand. Approximately 150 ± 10 μg of the dried sample was placed into a deactivated stainless-steel sample cup and pyrolyzed in the Py-GC/MS. For the Py-GC/MS experiments, the RS and EFB blends were prepared as per the procedures described in Section 2.1, ensuring homogeneous mixtures. Although the sample mass used for Py-GC/MS analysis was small (~150 μg) relative to the particle size (<1 mm), multiple replicate measurements were conducted for each blend, and consistent pyrolysis vapor compositions were obtained. This indicates that the sampled material was sufficiently representative of the bulk blend at the analytical scale. The micro-pyrolyzer exhibited a typical heating rate of approximately 500 °C s^{-1}. Prior to pyrolysis, the furnace was preheated to 500 °C. Helium was used as the carrier gas at a flow rate of 1.13 mL min^{-1}. Separation was achieved using

Table 1 A comparative summary of the three experimental setups, including their key features and purposes, the number of tests per sample, and a description of the individual and blend samples used

Experimental setup	Properties/key features	Purpose	Number of tests per sample	Individual or blend sample
Py-GC/MS	Micro-scale pyrolysis, high sensitivity, online GC-MS analysis	Identify volatile compounds released during pyrolysis	3	~0.1–0.2 mg of the individual or blended samples with particle size <1 mm
SPR	Well-controlled pyrolysis conditions, pyrolysis of a single particle (pellet)	Determination of char yields, continuous measurement and recording of CO and CO_2 gases	3	~150 mg pellets of individual or blended samples
FBR	Bench-scale fluidized bed reactor, continuous operation	Determining fast pyrolysis product yields and distributions, bio-oil production for analysis, continuous measurement and recording of CO and CO_2 gases	2	~20 g of the individual or blended samples with particle size <1 mm

a DB-5 capillary column (30 m length, 0.25 mm internal diameter, 0.25 μm film thickness). The injector and interface temperatures of the GC were maintained at 300 °C, while the detector temperature was set at 250 °C. The oven temperature program commenced with an initial hold at 40 °C for 2 min, followed by a ramp to 300 °C at a rate of 7 °C min^{-1}, and a final hold at 300 °C for 10 min. Mass spectrometry analysis was performed over the *m*/*z* range of 50–500 Da, and the detected compounds were identified using the NIST spectral library. Only compounds with detection quality greater than 85% were considered for classification. Each analysis was conducted in triplicate, with selectivity expressed as % peak area, and the standard error was 2–5%.

2.4. Fast pyrolysis experiments in a single-particle reactor

Fast pyrolysis of RS, EFB, and their three blends was carried out in a single-particle reactor (SPR) at 500 °C. A schematic diagram of the SPR and its accessories was reported previously.[6] Briefly, the reactor consists of a quartz-glass tube housed in an electrically heated ceramic furnace. A K-type thermocouple was used to monitor the temperature near the region in the SPR where pyrolysis of the sample occurs. Nitrogen gas was introduced in the reactor through five ports (front, back, sides, and bottom), with the flow rates controlled by mass flow controllers (Bronkhorst, Holland). Before each run, the furnace was preheated to 500 °C, and nitrogen gas was supplied at a total flow rate of 3.67 L min^{-1}. Approximately 150 mg of the biomass pellet (10 mm in diameter) was weighed and placed in a quartz-glass sample holder. The sample holder containing the pellet was mounted on a sample insertion probe, allowing the sample to remain in the SPR's colder zone until the reactor was fully purged of air. Thereafter, the sample was inserted into the hot reactor in approximately 2–3 s. After pyrolysis of the sample was complete, the sample insertion probe was retracted to the colder zone of the SPR and quenched in nitrogen to cool the residue (char including ash) left in the sample holder. The residue was then removed from the sample insertion probe and weighed to 0.1 mg accuracy. The CO and CO_2 gases formed during pyrolysis were continuously measured using a gas analyzer (AO2020 Continuous Emissions Analyzer, ABB, Germany), and the data were logged using a portable data logger. The char yields were determined gravimetrically, while the non-condensable gas yields, mainly CO and CO_2, were obtained from the analyzer measurements and the total nitrogen gas flow rate. The yields of the condensable pyrolysis vapors ('bio-oil') were calculated by difference. However, this method is expected to overestimate the actual bio-oil yields, as soot and some permanent gases (*e.g.*, H_2 and CH_4) formed during pyrolysis are included. Each experiment was repeated three times to ensure reproducibility, and the average values were reported. Further details of the SPR setup and the experimental procedures with it are available elsewhere.[6,29,30]

It should be noted that the SPR setup was not designed for bio-oil production; therefore, no bio-oil was produced during the SPR experiments. Instead, the system was used as a quick method to obtain preliminary estimates of potential bio-oil yields. Nevertheless, owing to its well-controlled gas atmosphere, the SPR is intended to complement the FBR results by offering mechanistic insight into the pyrolysis behavior of the individual biomasses and their blends.

2.5. Fast pyrolysis experiments in a fluidized bed reactor

Fast pyrolysis of the RS, EFB, and 50RS was conducted in a fluidized bed reactor (FBR) at 500 °C. Fig. 1 presents a schematic illustration of the reactor and its accessories. The setup consists of five main parts: a screw feeder, a reactor, a furnace, a bio-oil recovery system, and a gas analyzer. Compartment A of the reactor is the N_2 gas preheater; B is the compartment where pyrolysis of the sample occurs; C is the compartment for catalytic upgrading of the pyrolysis vapors (which was not used in this study); and D secures the reactor in the oven. For a typical fast pyrolysis run, about 40 g of the bed material (quartz sand with particle size 100–150 μm) was weighed and placed in compartment B. To retain the bed material in this compartment, two stainless steel wire meshes (63 μm mesh size) were secured between its top and bottom flanges. About 20 g of the dried sample was weighed and loaded into the screw feeder, which was purged several times with N_2 to remove air. N_2 gas was introduced into the reactor from the bottom at a flow rate of 1.3 L min^{-1} to ensure fluidization, and at 2 L min^{-1} through the screw feeder to facilitate sample feeding into the pyrolyzer. The minimum fluidization velocity for the bed material was 0.91 cm s^{-1}, while the superficial gas velocity was 5.88 cm s^{-1}. The fluidized bed temperature was the controlled pyrolysis temperature, 500 °C, whereas the VTL was kept at 400 °C. The three condensers were maintained at −20 °C using a cryostat cooler, and the bio-oils were collected in oil collectors fitted beneath the condensers. Two cotton filters were installed in series after the third condenser to capture oil aerosols, tiny oil droplets entrained with the pyrolysis gases. The concentrations of CO and CO_2 gases in the non-condensable gases were measured using a gas analyzer, and the data were logged using the portable data logger described in Section 2.4.

The bio-oil and biochar yields were determined gravimetrically, while the CO and CO_2 gas yields were obtained from the gas analyzer measurements. Each experiment was repeated two times, and the results were reported on a wt% dry biomass basis. A detailed description of the experimental setup and the experimental procedures with it is available from Aho *et al.*[31,32]

For clarity and better justification of the selected equipment, a comparative summary of the three experimental setups is presented in Table 1. The table highlights their main operational characteristics, experimental objectives, number of test repetitions, and the specific sample preparation conditions applied for each configuration.

2.6. Chemical composition of the bio-oils produced in the fluidized bed reactor

A Karl Fischer titrator (Metrohm 870 Titrino Plus) was used to determine the water content of the bio-oils. Most of the pyrolysis (reaction) water condensed in the first condenser and was collected in the first oil collector. The chemical composition of

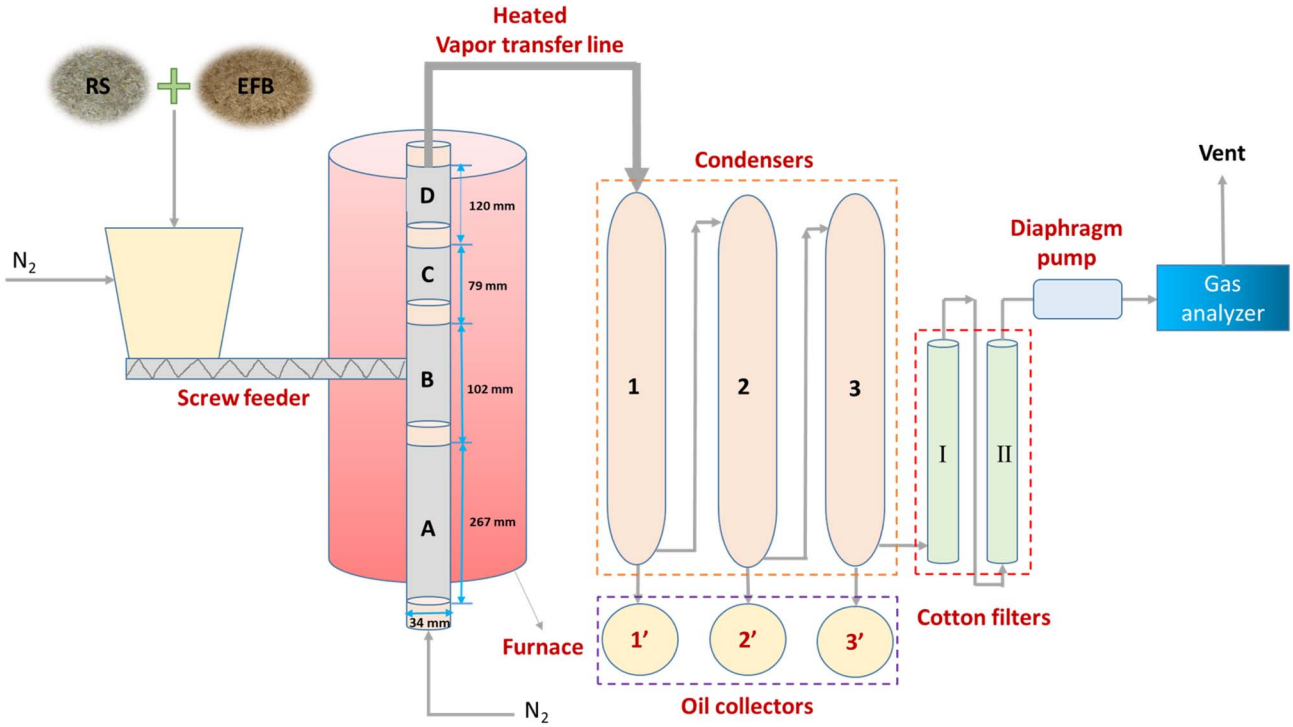

Fig. 1 Schematic diagram of the fluidized bed pyrolysis system.

the bio-oils was analyzed using a gas chromatograph (Shimadzu GC-2010 Plus) coupled with a mass spectrometer (GC-MS) and equipped with a RESTEK Rxi®-1 MS capillary column (30 m × 0.25 mm i.d. × 0.25 μm film thickness). The column consists of 100% dimethylpolysiloxane, representing a non-polar stationary phase suitable for the separation of complex bio-oil compounds. Prior to analysis with the GC/MS, the bio-oil samples were diluted with dichloromethane. The column was initially held at 45 °C for 2 min, and then ramped to 280 °C at 3 °C min^{-1}, and finally held at 280 °C for 10 min. A split ratio of 100 : 1 was applied. The injector, interface, and detector temperatures were set at 300 °C, 280 °C, and 250 °C, respectively. Mass spectra were matched against the NIST library, and only compounds with identification quality ≥85% were considered. Typically, 80–100 compounds were identified and categorized into the following functional groups: phenols, aromatic non-phenolics, cyclic oxygenates, furans, hydrocarbons, and hydrocarbon oxygenates. Compounds with lower match quality or multiple functional groups were assigned to broader categories. Selectivities for different compounds were determined from their GC/MS peak areas, and the results were reported as %peak area, with a standard deviation of 2–5%.

Furthermore, the chemical structures, *i.e.*, functional groups and chemical bonds, of the bio-oils produced from the individual RS and EFB samples and their 50 : 50 blends in the FBR were identified using a Cary 630 Fourier transform infrared (FTIR) spectrometer (Agilent Technologies), equipped with an attenuated total reflectance (ATR) module. The spectra were collected over the range of 4000–600 cm^{21} with a resolution of 2 cm^{-1}.

2.7. Influence of co-pyrolysis of RS and EFB on product yields and composition

The effect of mixing the RS and EFB samples on pyrolysis product yields and composition was assessed by applying the mixture rule[10] given in eqn (1). In eqn (1), X_{RS} and X_{EFB} represent the respective fractions of RS and EFB in the mixture, while Y_{RS} and Y_{EFB} denote the experimental product yields or compositions obtained from the pyrolysis of the individual biomasses. The influence of blending the biomasses is described by a parity plot of the $Y_{Calculated}$ *vs.* $Y_{Experimental}$.

$$Y_{calculated} = X_{RS}\ Y_{RS} + X_{EFB}\ Y_{EFB} \quad (1)$$

3. Results and discussion

3.1. Chemical composition of the RS and EFB

Table 2 presents the chemical composition of RS and EFB from Tiwari *et al.*[6] The lower volatile matter and cellulose contents, coupled with the higher ash content, of the RS make it a less suitable feedstock for bio-oil production than the EFB. It is well established that biomass with low volatile matter and cellulose contents, as well as high ash contents-especially alkali and alkaline earth metals (AAEMs), reduce the bio-oil yields during pyrolysis.[33] AAEMs reduce bio-oil yields through their catalytic effect, promoting secondary cracking reactions in the vapor-phase pyrolysis products.[34] Thus, blending the RS with a better-quality biomass feedstock, *e.g.*, EFB, is expected to enhance the yield and quality of bio-oil and the overall economic performance of the pyrolysis process.

Table 2 Chemical composition of the biomass feedstocks[6]

	RS	EFB
Elemental composition (wt% biomass, dry basis)		
C	40.2	47.1
H	5.3	5.9
N	0.5	0.4
S	0.3	0.1
K	1.6	1.2
Na	0.4	0.02
Ca	0.3	0.1
Mg	0.2	0.1
Si	4.8	0.3
Al	0.05	0.003
Fe	0.1	0.02
P	0.05	0.04
Cl	0.4	0.2
Proximate analysis		
Ash content (wt% biomass, dry basis)	9.8	0.9
Volatile matter (wt% biomass, dry ash-free basis)	85.4	82.7
Fixed carbon (wt% biomass, dry ash-free basis)	14.6	17.3
Biochemical composition (wt% biomass, dry basis)		
Cellulose (glucose equivalent)	40.5	46.7
Hemicellulose (xylan/xylose equivalent)	25	27.7
Lignin	19.3	21.7
LHV (MJ kg^{-1}, dry basis)	14.3	17.4

3.2. TGA results

Fig. 2 shows the sample mass loss (TG) and differential mass loss (DTG) profiles of the individual biomass and their blends from the TGA experiments. Three stages of mass loss are observed: moisture removal (stage 1), "active" pyrolysis (stage 2), and "passive" pyrolysis (stage 3). Moisture, 7–8 wt%, was removed from the samples below 150 °C. Significant sample mass loss, 55–65 wt%, occurred between 150 °C and 450 °C during the active pyrolysis, stage 2. This stage is primarily ascribed to the decomposition of cellulose and hemicellulose components of the samples. The decomposition temperatures corresponding to the maximum mass loss rates were 324 °C and 320 °C for EFB and RS, respectively. In stage 3, above 450 °C, the mass loss slowed down due to the slow thermal decomposition of lignin. Literature also shows that lignin thermal degradation under inert gas conditions occurs over a wide temperature range of 150–850 °C,[35] while cellulose and hemicellulose decompose at a lower temperature range, 150–450 °C.[35] Furthermore, the results shown in the figures reveal that the TG and DTG curves for the RS-EFB blends fall approximately between the corresponding curves for the pure RS and pure EFB. This observation suggests that the pyrolysis behavior of the blends largely adheres to the mixture rule.

3.3. Py-GC/MS results

The Py-GC/MS identified various compounds present in the pyrolysis vapors. The salient compounds were grouped into phenols (P), linear oxygenates (L-O), cyclic oxygenates (Cy-O), aromatic oxygenates (Ar-O), furans (F), and others mainly nitrogen- and sulfur-containing compounds. The classification was based on the information in the literature for biomass pyrolysis using Py-GC/MS.[36,37] The list of major chemical compounds with their functional groups and the total ion chromatograms (TICs) obtained from the Py-GC/MS are provided in Tables S1–S4 and Fig. S1 of the SI, respectively.

Fig. 3(a) shows the selectivities for the various functional groups in the pyrolysis vapors, and Fig. 3(b) displays the parity chart comparing the calculated and experimental selectivities for the RS-EFB blends. As seen in Fig. 3(a), linear oxygenates are the dominant products (~55–65%) in the pyrolysis vapors from the RS, EFB, and their mixtures. The levels of cyclic oxygenates and phenols accounted for 15–25% and 5–25%, respectively. The linear and cyclic oxygenates were higher in the RS pyrolysis vapors than in the EFB, likely due to the higher concentration of AAEMs in the RS. Previous studies[38] also reported that AAEMs catalyze the conversion of larger molecules, such as anhydrosugars, into lighter, linear oxygenates containing carbonyl and carboxyl functional groups during pyrolysis. The linear oxygenates are mainly composed of pentadecanoic acid ($C_{15}H_{50}O_2$), acetaldehyde (C_2H_4O), methyl glyoxal ($C_3H_4O_2$), acetic acid ($C_2H_4O_2$), and butanoic acid ($C_4H_8O_2$), and these compounds primarily originate from the decomposition of cellulose and hemicelluloses. The level of phenolic compounds was higher in the EFB pyrolysis vapors than in the RS, probably due to the higher lignin content of the EFB (Table 2). The major phenolic compounds identified by the Py-GC/MS were simple phenols (phenol), methoxy phenols, and 2-methoxy-4-vinylphenol. The RS produced squalene, a high-molecular-weight hydrocarbon, also likely originating from lignin.[39]

The chemical composition of the RS bio-oil was dominated by linear oxygenates (64%), primarily light acids and ketones, followed by cyclic oxygenates (25.8%) and phenolic compounds (6.7%). This distribution aligns with the typical product spectrum of RS pyrolysis oils, which largely originate from the thermal decomposition of carbohydrates (cellulose and hemicellulose) and lignin.[40] The relative peak area of levoglucosan obtained in this study for the RS (3.4%) was lower than the value reported in the literature (11.3%).[40] This difference can be attributed to the higher ash content particularly AAEMs present in the RS used in this work. AAEMs are known to catalyze fragmentation and secondary reactions, thereby suppressing levoglucosan formation during cellulose depolymerization. In contrast, the bio-oil produced from EFB contained a high proportion of linear oxygenates (55.2%) and phenolic compounds (23.5%). This compositional trend is consistent with previous studies on EFB pyrolysis, which report light oxygenates (30%), heavy oxygenates (25%), and phenolics (40%) as the major product groups.[41]

Fig. 3a and b reveal an interesting observation: the pyrolysis vapor composition of the RS-EFB blends varied proportionally with the mixing ratio. For instance, the amount of phenolic compounds in the pyrolysis vapors increased and those of the linear, cyclic, and aromatic oxygenates decreased as the percentage of EFB in the mixture increased. The increase in the concentration of phenolic compounds resulting from the mixing can be beneficial if there is market need to produce bio-oil

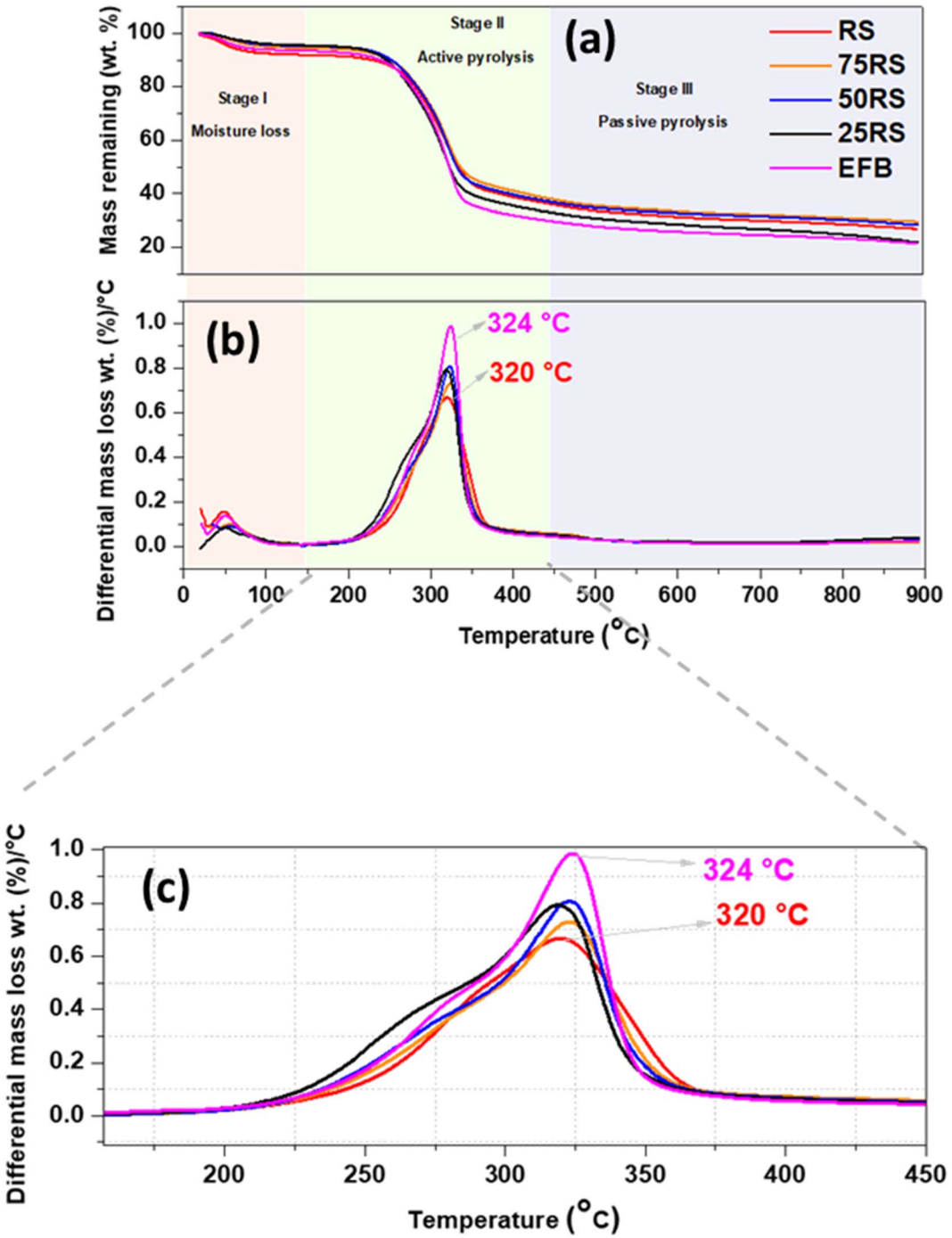

Fig. 2 TGA (a), DTG (b), and magnified version of the DTG (c) of the "active" pyrolysis stage for RS, EFB, and their blends.

from the RS with high phenolic selectivity. Additionally, the mixing ensures a sustainable feedstock supply for the phenolics production from the bio-oil.

3.4. Pyrolysis product yields and distribution from the single-particle reactor

Fig. 4(a) shows product yields and distribution from pyrolysis of the RS, EFB, and their blends at 500 °C in the SPR. Fig. 4(b) shows the parity plot for the calculated *vs.* experimental yields for the biomass blends. Pyrolysis of the RS produced a higher char yield than the EFB, owing to its higher AAEM content, which favours char formation. The char yield results agree with the literature reports for RS[42] and EFB.[43] On the other hand, the EFB produced a higher condensables ("bio-oil") yield than the RS, whereas the CO and CO_2 yields for both samples were approximately the same. The higher condensables yield obtained from the EFB can be attributed to its high volatile matter content. However, the "bio-oil" yields from the SPR were

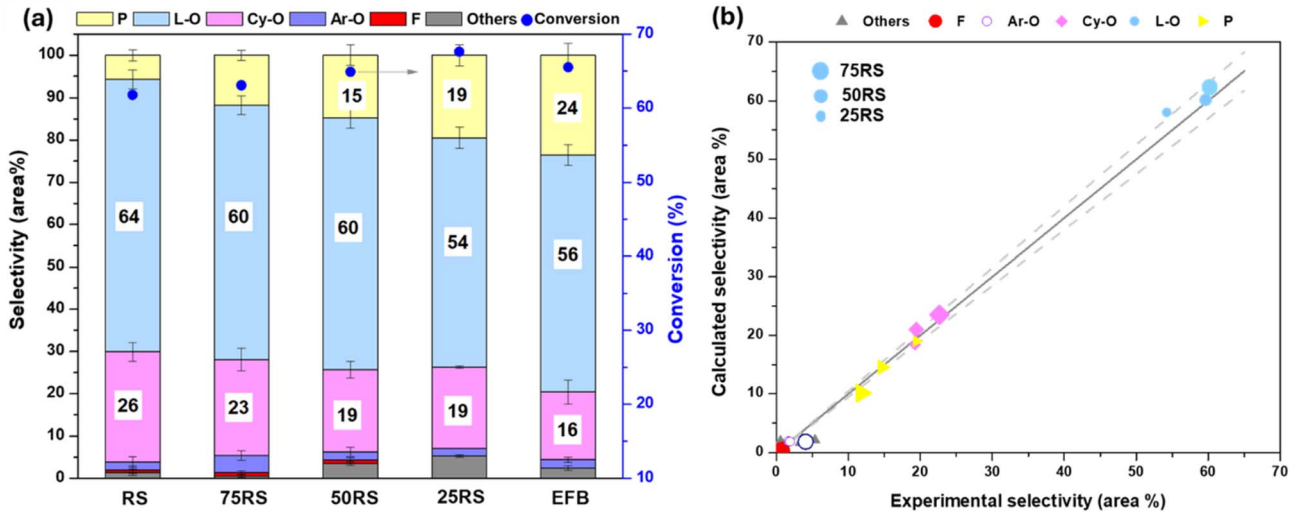

Fig. 3 Selectivity (area%) (a) and parity chart (b) for the pyrolysis of RS, EFB, and their three blends at 500 °C in the Py-GC/MS. The results represented by blue dots (•) given on the secondary *Y*-axis in (a) are percentage conversions of the RS and EFB samples and their blends in the Py-GC/MS.

overestimated, as soot and permanent gases (*e.g.*, H_2, CH_4, and others) were included in the condensables fraction, as described in Section 2.4. Heavy soot deposits were observed in the gas transfer line between the reactor and the gas analyzer. These deposits partly originated from the carryover of soot particles formed during pyrolysis of the biomass pellets in the reactor. The soot deposits might have also been formed from the backward Boudouard reaction ($2CO(g) \rightarrow C(s) + CO_2(g)$), which occurs spontaneously at temperatures ≤300 °C. The temperature of the gas transfer line close to the reactor, where heavy soot deposit formation occurred, was mostly ≤300 °C for the pyrolysis experiments carried out at 500 °C. Thus, soot formation *via* the Boudouard reaction not only overestimated the actual bio-oil yields but also might have introduced uncertainties in the CO and CO_2 gas yields.

As can be seen from Fig. 4(b), the product yields obtained from pyrolysis of the biomass mixtures agree with the calculated values. In other words, increasing the fraction of EFB in the mixture decreased the char yields and increased the "bio-oil" yields and *vice versa*. This indicates that the individual biomasses in the mixture behaved as if they were pyrolyzed independently. Thus, the yield and quality of bio-oil derived from a low-quality biomass can be enhanced by blending it with a higher-quality biomass, with the extent of improvement increasing proportionally with the fraction of the higher-quality biomass in the mixture. However, due to the limitations of the SPR for bio-oil production (as described in Section 2.4), it is not

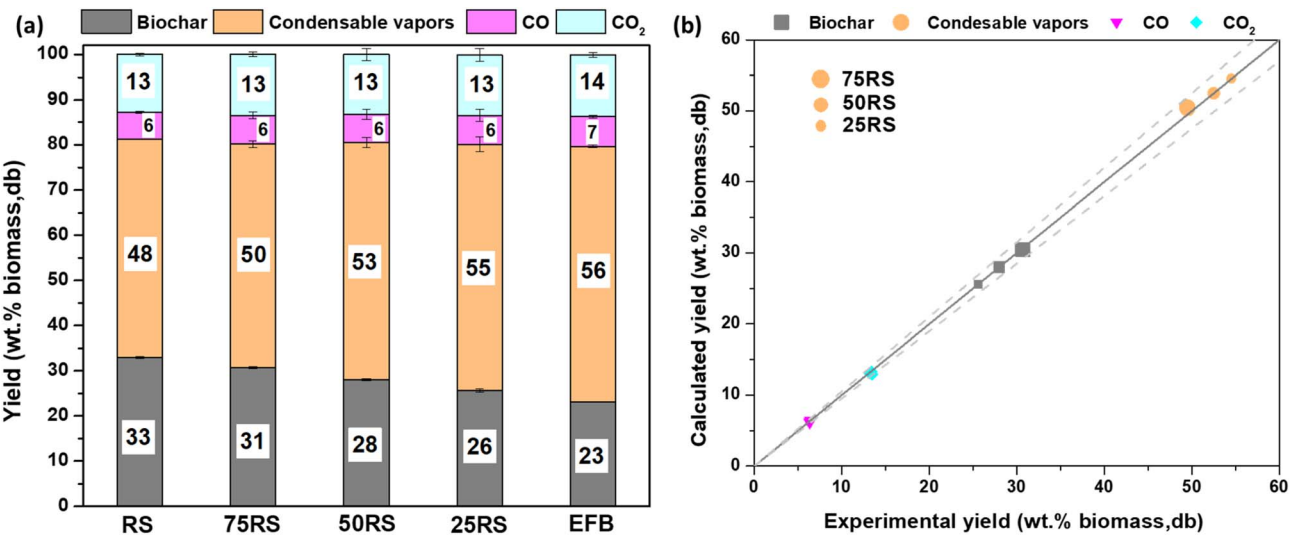

Fig. 4 Product yield and distribution (a) and parity plot (b) for pyrolysis of the RS, EFB, and their three blends at 500 °C in the single-particle reactor.

possible to reliably quantify bio-oil yields or assess their quality based on the SPR results. Consequently, all discussions related to bio-oil yields and quality improvements are based on the FBR and Py-GC/MS results, where representative yield determinations and detailed chemical analyses were conducted.

3.5. Pyrolysis product yields and distribution from the fluidized bed reactor

Fig. 5(a) shows product yields obtained from fast pyrolysis of the individual biomass samples and their blend (50RS) in the FBR at 500 °C. Fig. 5(b) shows the parity chart for the calculated *vs.* experimental pyrolysis product yields. For each sample, the results given in the figures are average values of two pyrolysis runs. The deviations of the pyrolysis product yields from the average values were ≤1%, indicating the repeatability of the pyrolysis experiments in the FBR. The results also show a good mass balance closure, 97–99%. The "Balance" given in the figures is due to unaccounted biochar and bio-oils left adhering to the reactor walls and gases, *e.g.*, H_2 and CH_4, in the non-condensable pyrolysis gases, which were not analysed.

As shown in the figures, the EFB produced higher water-free bio-oil and lower biochar yields than the RS, primarily due to its lower ash content and higher volatile matter content. The CO and CO_2 gas yields from both samples were the same. The pyrolysis water yield from the EFB was slightly higher than that from the RS, likely due to differences in their chemical compositions. Fast pyrolysis of the RS at 500 °C in the FBR produced a total liquid yield (organic fraction plus pyrolysis water) of 41 wt%, which is consistent with the 43 wt% reported in the literature for fast pyrolysis of RS in a fluidized bed reactor operated at the same temperature.[28] The corresponding biochar and non-condensable gas yields (30 wt% and 26 wt%, respectively) also agree well with previously reported values of 27 wt% for biochar and 23 wt% for non-condensable gases.[28] The minor variations in the product distributions can be attributed to differences in RS particle size and the biochar removal systems used. For the EFB, the total liquid, biochar, and on-condensable gas yields obtained in this work 50, 23, and 26 wt%, respectively are in close agreement with the corresponding literature values of 49, 25, and 24 wt%.[44] For the 50/50 blend (50RS), the pyrolysis product yields are very similar to the average yields from the individual samples, suggesting that the biomasses in the mixture pyrolyzed independently. This observation is consistent with the results obtained from the Py-GC/MS and SPR.

Comparison of the bio-oil yields obtained from fast pyrolysis of the samples in the FBR (Fig. 5(a)) with the respective results from the SPR (Fig. 4(a)) shows lower bio-oil yields from the FBR. In practice, however, higher bio-oil yields from the FBR are expected due to the high heat-transfer rates in fluidized-bed reactors. The higher "bio-oil" yields reported for the SPR are primarily due to the yield-determination method, which overestimates actual yields. As discussed in Section 2.4, the overestimation arises from considering soot and permanent gases (*e.g.*, H_2 and CH_4) as condensables. A similar explanation could be given for the lower CO and CO_2 gas yields obtained from pyrolysis of the samples in the SPR than in the FBR. Nonetheless, the results from the FBR show that co-pyrolysis of the RS with the EFB improves bio-oil yield compared to that from pyrolysis of the RS alone.

3.6. Chemical composition of the bio-oils

Fig. 6(a) illustrates the chemical composition of the bio-oils produced in the fluidized bed reactor (FBR). The functional groups in the bio-oils were categorized using the same classification approach used for the Py-GC/MS analysis described in Section 3.3. Fig. 6(b) compares the experimentally determined selectivities of the compound groups in the bio-oil derived from the 50RS blend with those predicted by calculations. The chemical compounds in the bio-oils, categorized by functional groups, along with their total ion chromatograms (TICs), are provided in Tables S5–S7 and Fig. S2, respectively, of the SI.

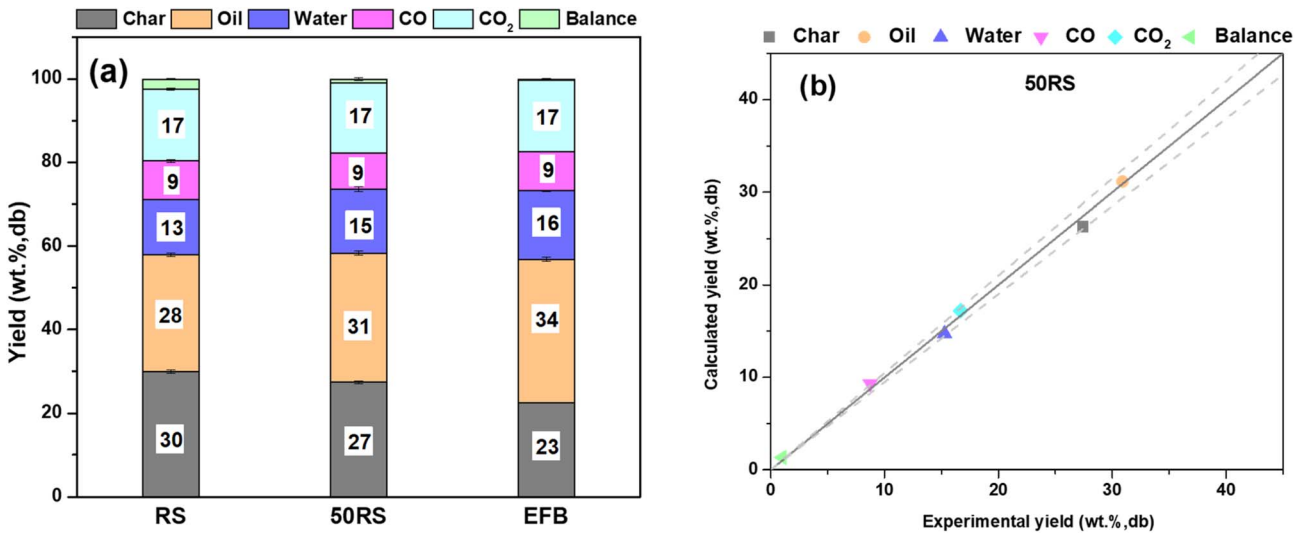

Fig. 5 Product yields (a) and parity plot (b) for fast pyrolysis of the RS, EFB, and their 50/50 blend at 500 °C in the fluidized bed reactor.

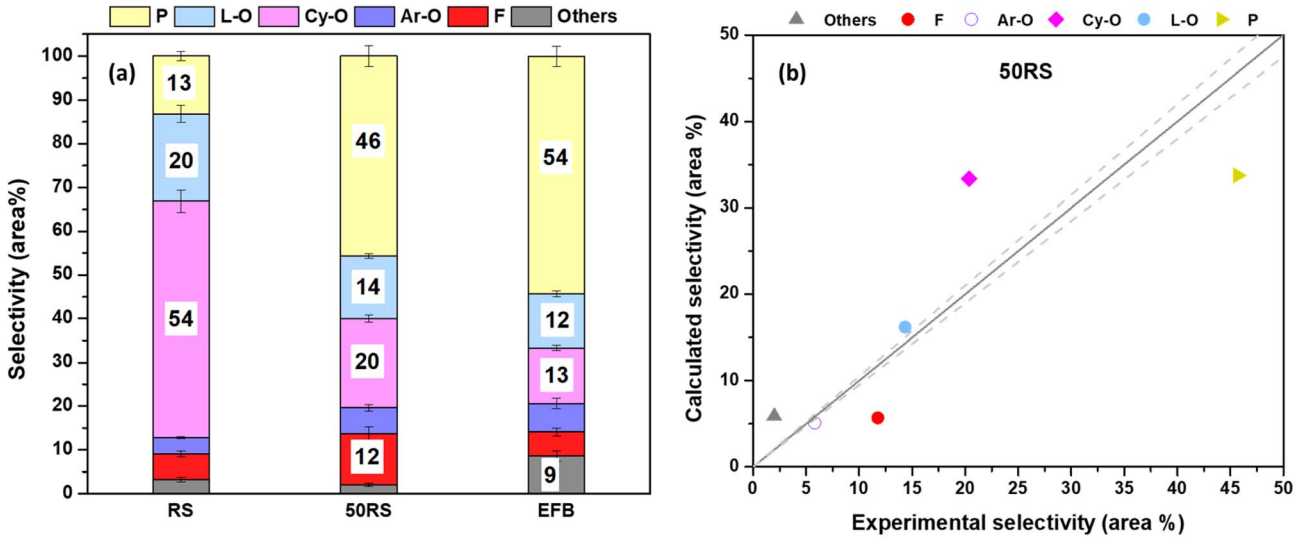

Fig. 6 Selectivity for primary functional groups in bio-oils (a) and their parity plot (b) for the bio-oils obtained from pyrolysis of RS, EFB, and their 50/50 blend in the fluidized bed reactor at 500 °C.

Fig. 6(a) shows distinct differences in the chemical composition of the bio-oils derived from RS and EFB, arising from variations in the chemical and biochemical composition of the biomasses. Both the RS and EFB bio-oils were rich in oxygenated compounds and phenols; however, the RS bio-oil was dominated by cyclic oxygenates while the EFB bio-oil contained primarily phenolic compounds. The main cyclic oxygenates detected in the RS bio-oil were 3-cyclopentene-1-acetaldehyde, 2-cyclopenten-1-one and its oxo derivative, as well as 2-hydroxy-3-methyl compounds. In contrast, linear oxygenates, such as 1-hydroxy-2-butanone and pentanal, were present in the bio-oil in smaller quantities. The phenolic compounds in the EFB bio-oil consisted mainly of simple phenols, alkyl phenols, and methoxy phenols.

Compared to pyrolysis vapors generated in the Py-GC/MS, the bio-oils produced in the FBR from both the RS and EFB samples contained a higher proportion of cyclic oxygenates, whereas the pyrolysis vapors produced in the Py-GC/MS from these samples were predominantly rich in linear oxygenates. This difference is probably due to the longer vapor residence time (~2 s) in the FBR, leading to greater secondary vapor-phase cracking reactions. Also, during pyrolysis in the FBR, the char formed remains in the reactor for the entire pyrolysis duration (25–30 min). This prolonged contact of the char with the pyrolysis vapors promotes vapor cracking, cyclization, α-O-4 and β-O-4 bond cleavage, and β-scission, collectively enhancing the formation of cyclic oxygenated compounds. In contrast, the vapor residence time in the Py-GC/MS is extremely short typically on the order of milliseconds minimizing vapor-phase secondary cracking reactions. Thus, the primary pyrolysis products, such as aldehydes and ketones, are detected by the GC/MS (Fig. 3(a) and Tables S1–S5 of the SI).

Blending the RS with the EFB increased the concentration of phenolic compounds in the bio-oil produced from the mixed biomass compared to that from the RS alone. Thus, mixing of the RS with the EFB may be industrially relevant, for example, for the production of a specific phenolic compound for platform chemicals.[20] Moreover, the selectivity to furans (mainly 5-methyl 2-furan carboxaldehyde ($C_6H_6O_2$), 1-(2-furanyl)-ethanone ($C_6H_6O_2$), and tetrahydro-2-furan methanol ($C_5H_{10}O_2$)) increased in the bio-oil with increasing proportion of EFB in the biomass mixture (Fig. 3 and 6). However, further work is needed, as the results shown in the figures are semi-quantitative.

Additionally, Fig. S3 (SI) shows the FTIR spectra of the bio-oils produced in the FBR at 500 °C from the RS, EFB, and their 50/50 blend (50RS). All the bio-oils exhibited O–H (~3400 cm^{-1}) and C–H (~2900 cm^{-1}) bond stretches. The RS-derived bio-oil showed distinct bands corresponding to secondary amines and cyclic ethers (1500–1250 cm^{-1}), while the EFB bio-oil displayed more pronounced peaks associated with aromatic amines and C–Cl bonds (~1350 and 800–600 cm^{-1}). In contrast, the bio-oil obtained from the 50RS blend showed intermediate structural characteristics, featuring carboxylate and aromatic bands (~1700–1500 cm^{-1}), indicating a combination of chemical structures from both biomasses.

3.7. Reaction mechanisms for the pyrolysis of the biomass blends

The different pyrolysis techniques used (Py-GC/MS, SPR, and FBR) may lead to variations in pyrolysis reaction mechanisms, resulting in differences in the pyrolysis product yields and composition. For example, primary pyrolysis is the dominant mechanism in Py-GC/MS because of the high heating rates in the system. The smaller sample size (~100–150 μg), finer particles (≤1 mm), and shorter pyrolysis residence time in the reactor enhanced heat transfer rates in the Py-GC/MS system. These conditions promoted rapid breakdown of the samples into char and primary pyrolysis vapors in the kinetic-controlled reaction regime. In the FBR, however, the retention of char in

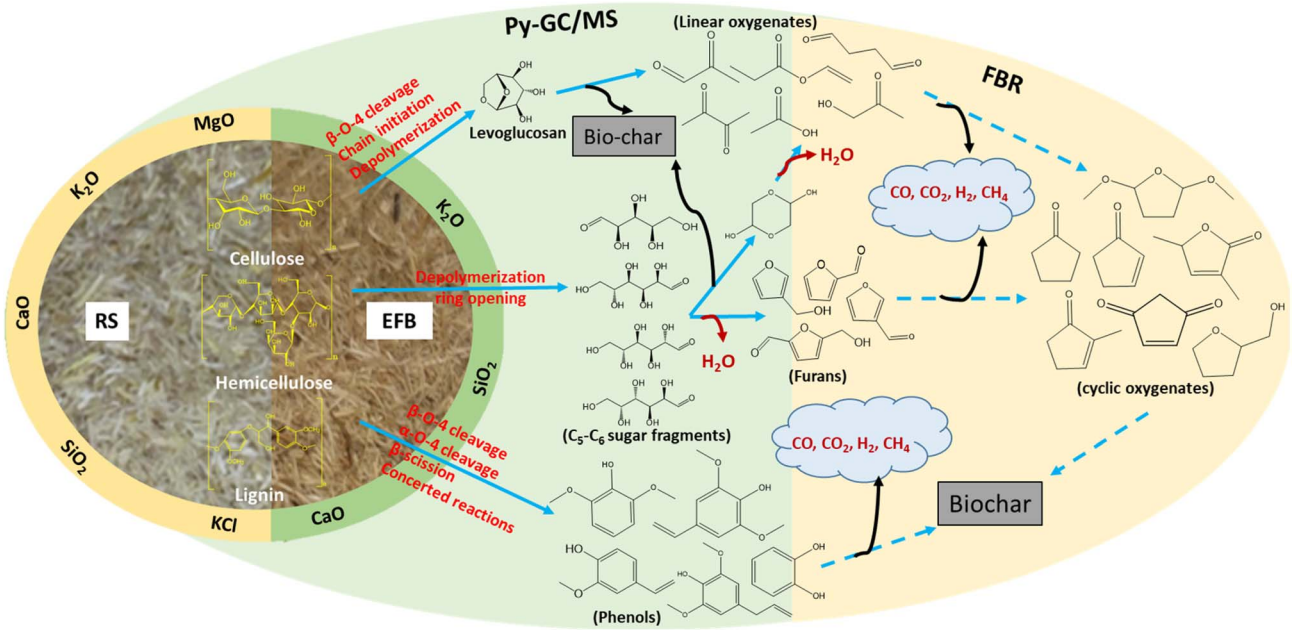

Fig. 7 Plausible reaction mechanism for co-pyrolysis of RS and EFB in the Py-GC/MS and fluidized bed reactor at 500 °C.

the reactor during pyrolysis and the longer residence time of the pyrolysis vapors in the reactor might have promoted secondary cracking reactions in the vapor phase product. This, in turn, might have further broken down the primary pyrolysis vapor products into lighter compounds, such as phenols, organic acids, and ketones. Fig. 7 shows schematically the plausible reaction mechanisms involved in the pyrolysis of the RS and EFB blends in the Py-GC/MS and FBR systems. The pyrolysis behavior of the biomass blends in both Py-GC/MS and FBR highlights that blending primarily affects lignin decomposition, while cellulose and hemicellulose decomposition remains largely unaffected. This is corroborated by the mass loss data, illustrated in Fig. 2, which shows that individual biomass samples and their blends exhibited similar mass loss patterns within the cellulose and hemicellulose decomposition temperature ranges. These findings suggest that lignin is the main component affected by biomass blending, whereas the decomposition of cellulose and hemicellulose remains largely consistent regardless of the blend composition.

Lignin breakdown has a significant impact on the concentration of phenolic compounds in the pyrolysis bio-oils from the RS and EFB blends. For this, the ratio of syringol (S) to guaiacol (G) to hydroxyphenol (H) in the bio-oils or pyrolysis vapors is a good indicator. The ratio increased in the pyrolysis of both the individual and blended samples in the Py-GC/MS and FBR. Fig. 8 shows the reaction mechanisms for lignin decomposition during pyrolysis of biomass blends in the Py-GC/MS and FBR, and the S : G : H ratios in the pyrolysis vapors/oils for the different blends. The increase in the S to G ratio of the pyrolysis vapors produced in the Py-GC/MS is attributed to the cellulose and lignin interactions during pyrolysis of the biomass blends. Liu *et al.*[45] also studied the phenolic contents of bio-oils produced from pyrolysis of model compounds (cellulose, xylan, and lignin) at different blending ratios. They reported that the phenol and G-phenol yields increased due to mixing, while the H-phenol yields remained constant. The substantial increase in H-phenol formation for the RS-EFB blend in the FBR can be attributed to secondary cracking reactions in the primary pyrolysis vapor-phase product, promoting the demethoxylation of the S and G units into simpler H-type phenols. This process is further enhanced by the longer vapor residence time in the FBR, as well as the catalytic effect of AAEMs.

3.8. Influence of intraparticle heat transfer and particle size on fast pyrolysis product yields and distribution

The three reactor configurations investigated in this work represent fundamentally different intraparticle heat transfer and reaction regimes, arising from differences in particle size, geometry, and reaction environment.[46] These differences govern characteristic heat transfer length scales, internal temperature gradients, vapor residence times, and ultimately the balance between primary and secondary pyrolysis chemistry.

In the Py-GC/MS system, the sample mass is extremely small (~150 μg) and subjected to a nominal heating rate of ~500 °C s^{-1}. The characteristic heat transfer length is on the micrometer scale, rendering internal conductive resistances negligible. Under these conditions, particles can be reasonably approximated as nearly isothermal throughout heating and devolatilization. As a result, the measured products predominantly reflect intrinsic, kinetically controlled primary decomposition of biomass constituents. Vapor residence times are very short, and opportunities for secondary cracking, dehydration, or vapor–solid interactions are minimal.[40] Consequently, this configuration closely approaches an ideal fast pyrolysis process dominated by primary reaction chemistry, yielding very high

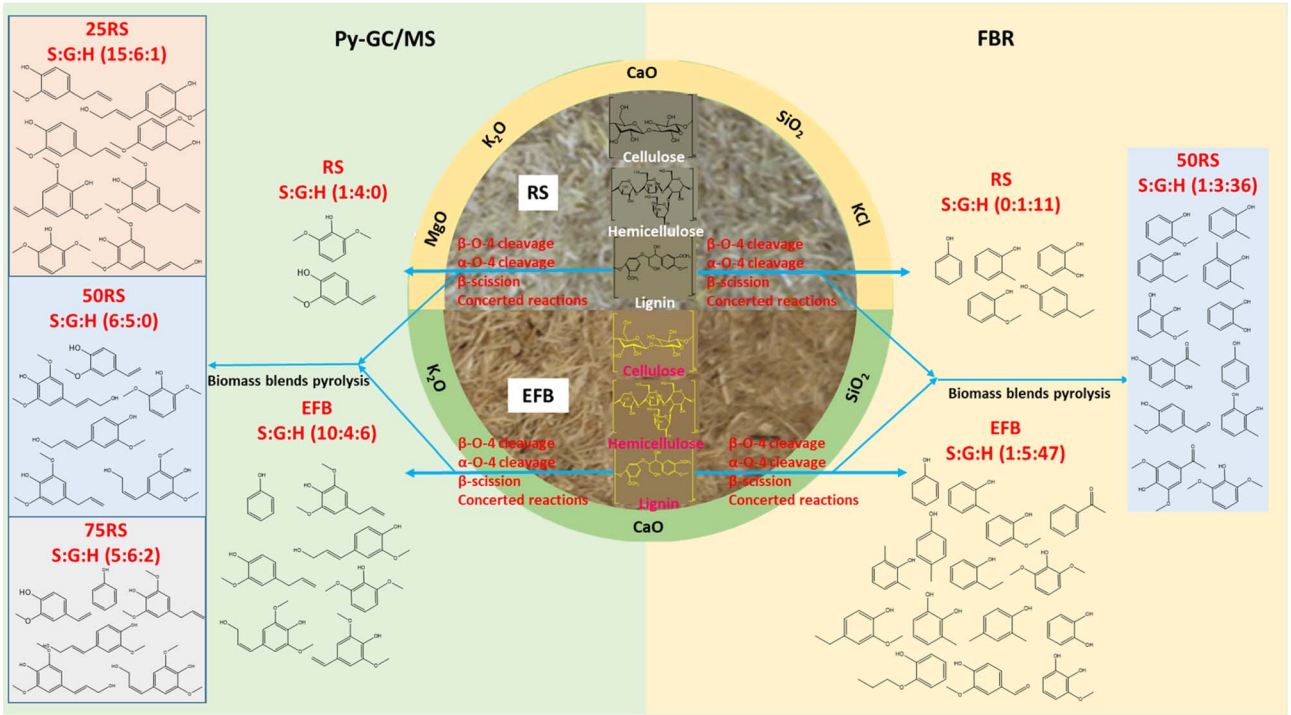

Fig. 8 Plausible reaction mechanisms for lignin decomposition during co-pyrolysis of RS and EFB in the Py-GC/MS and FBR at 500 °C, along with typical syringol (S) to guaiacol (G) to hydroxyphenol (H) ratio in the bio-oil.

vapor conversion (~90–99%), low char formation (~1–10%), and condensates rich in oxygenated species.

In contrast, the SPR employs cylindrical pellets of approximately 10 mm diameter (~150 mg), introducing a fundamentally different thermal regime. At this scale, intraparticle heat transfer becomes a governing factor. Both experimental and modeling studies demonstrate that large particles develop substantial radial temperature gradients during rapid external heating.[46] Even when the furnace heating rate is high, the effective heating rate at the pellet center can be one to two orders of magnitude lower due to internal conductive limitations. This produces a moving reaction front: the outer shell reaches pyrolysis temperatures first and undergoes devolatilization, secondary cracking, dehydration, and aromatization, while the core remains at a lower temperature and reacts more slowly. Vapors generated in the less-hot interior part of the particle must pass through the hotter outer layer, promoting further cracking and deoxygenation. As a result, vapor conversion decreases (~67–77%), while gas and char fractions increase (~23–33%), and the condensable products exhibit greater degrees of secondary transformation. Explicit consideration of dimensionless parameters, such as the Biot number and the characteristic conduction time, would further clarify that the SPR operates in a conduction-limited regime.[47,48]

The fluidized bed reactor (FBR) represents an intermediate but distinct regime. Although the total biomass feed is larger (20 g), the governing parameter for intraparticle effects is the individual particle size distribution, typically in the millimeter range (~1–3 mm). Intense gas–solid mixing and high external heat transfer coefficients minimize external heat transfer resistance, so intraparticle conduction again becomes the principal limitation. Compared to 10 mm pellets, millimeter-scale particles develop less severe internal temperature gradients, and their surfaces may approach fast pyrolysis conditions. Nevertheless, delayed core heating and moderate internal gradients can still occur, especially for larger or denser particles. Accordingly, the FBR exhibits intermediate product distributions, with liquid yields of ~41–50 wt%, gas yields of ~25–26 wt%, and bio-oils reflecting partial secondary reactions and moderate deoxygenation.

Overall, the pronounced differences in particle size and thermal transport among the Py-GC/MS, SPR, and FBR systems place each reactor in a distinct intraparticle heat transfer regime: (i) nearly isothermal, kinetically controlled primary pyrolysis (Py-GC/MS); (ii) strongly conduction-limited, gradient-driven secondary conversion (SPR); and (iii) externally well-mixed but moderately conduction-influenced behavior (FBR). These regimes critically influence the fast pyrolysis product yields and composition for both individual RS and EFB samples and their blends. Therefore, nominal reactor temperature or vapor residence time alone is insufficient to rationalize the observed trends; particle-scale heat transfer and internal temperature evolution must be explicitly considered when comparing pyrolysis performance across reactor configurations.

4. Conclusions

This study unravelled the impact of biomass blending on pyrolysis product yields and composition using Py-GC/MS, a single-particle reactor (SPR), and a fluidized-bed reactor (FBR)

operated at 500 °C. Rice straw (RS), empty fruit bunch (EFB), and their mixtures 25% RS + 75% EFB, 50% RS + 50% EFB, and 75% RS + 25% EFB (dry biomass weight basis) were used. The results show that the EFB produced higher bio-oil (condensable) yields than the RS, with 56 wt% in the SPR and 50 wt% in the FBR for the EFB, compared to 48 wt% and 46 wt% for the RS in the respective reactor systems. Conversely, biochar yields were greater for the RS than for the EFB in both the SPR and FBR systems. The lower bio-oil/condensable and higher biochar yields observed for the RS than for the EFB can be attributed to its higher ash content, particularly alkali and alkaline earth metals. Both the RS and EFB pyrolysis vapors/bio-oils were composed primarily of oxygenated compounds (linear and cyclic) and phenolics. However, the RS-derived vapors/bio-oils contained higher levels of oxygenates, whereas those from the EFB were richer in phenolic compounds. Variations in product yields and distribution among the three reactors are primarily due to differences in their design, which affected pyrolysis vapor residence times, sample sizes, intraparticle heat transfer, and heating rates. Co-pyrolysis of the RS and EFB revealed that the product yields and composition generally adhered to the mixture rule, each biomass pyrolyzed independently of the blending ratio, and both the yields and composition were proportional to the mixing ratio. Nevertheless, the findings of this study suggest that co-pyrolysis of biomass residues with diverse chemical compositions and availability may improve product yields and quality, thereby enhancing the overall sustainability of the fast pyrolysis process.

Author contributions

Tiwari Mahendra contributed to formal analysis, investigation, methodology development, validation, visualization, drafting the original manuscript, and reviewing and editing. Dirbeba Meheretu Jaleta contributed to conceptualization, formal analysis, investigation, methodology development, visualization, drafting of the original manuscript, supervision, and reviewing and editing. Ruozzi Alessandro was involved in formal analysis, investigation, methodology development, and validation. Lehmusto Juho contributed to analysis, investigation, and reviewing and editing of the manuscript. Yrjas Patrik contributed to conceptualization, funding acquisition, resource provision, supervision, and reviewing and editing of the manuscript. Vinu Ravikrishnan was responsible for conceptualization, formal analysis, funding acquisition, methodology development, resource provision, supervision, visualization, drafting the original manuscript, and reviewing and editing.

Conflicts of interest

The authors declare no competing financial interest.

Data availability

All supporting data are included in this manuscript or its supplementary information (SI). Additional data are available from the corresponding authors on reasonable request. Supplementary information is available. See DOI: https://doi.org/10.1039/d5se01603g.

Acknowledgements

This study was conducted within the project "Thermal Conversion of Challenging Indian and Finnish Feedstocks with a Focus on Pyrolysis," which received seed funding through the India Pilot initiative of the Finnish Ministry of Education and Culture. The India Pilot Network FICORE (Finnish Indian Consortia for Research and Education), coordinated by Aalto University, includes 38 higher education institutions from Finland and India.

References

1 Biomass Energy, https://education.nationalgeographic.org/resource/biomass-energy/, accessed September 12, 2024.
2 M. F. Demirbas, M. Balat and H. Balat, *Energy Convers. Manage.*, 2009, **50**, 1746–1760.
3 J. Ben-Iwo, V. Manovic and P. Longhurst, *Renew. Sustain. Energy Rev.*, 2016, **63**, 172–192.
4 D. C. Makepa and C. H. Chihobo, *Biomass Convers. Biorefinery*, 2025, **15**, 11397–11419.
5 E. M. El-Fawal, A. M. A. El Naggar, A. A. El-Zahhar, M. M. Alghandi, A. S. Morshedy, H. A. El Sayed, A. elshifa and M. E. Mohammed, *RSC Adv.*, 2025, **15**, 11942–11974.
6 M. Tiwari, M. J. Dirbeba, J. Lehmusto, P. Yrjas and R. Vinu, *J. Anal. Appl. Pyrolysis*, 2024, **177**, 106355.
7 N. F. Azman, T. Katahira, Y. Nakanishi, N. Chisyaki, S. Uemura, M. Yamada, K. Takayama, I. Oshima, T. Yamaguchi, H. Hara and M. Yamauchi, *Clean.Circ.Bioecon.*, 2023, **6**, 100058.
8 H. Onyeaka, T. Miri, K. C. Obileke, A. Hart, C. Anumudu and Z. T. Al-Sharify, *Carbon Capture Sci. Technol.*, 2021, **1**, 100007.
9 M. Shahbaz, A. AlNouss, I. Ghiat, G. Mckay, H. Mackey, S. Elkhalifa and T. Al-Ansari, *Resour. Conserv. Recycl.*, 2021, **173**, 105734.
10 M. Tiwari and R. Vinu, *Process Saf. Environ. Prot.*, 2024, **190**, 606–621.
11 Z. Gao, D. Zeng, S. Wu, S. Ren, F. Zhou, M. Gao, F. Song, Y. Zhai and R. Xiao, *Sustain. Energy Fuels*, 2023, **7**, 2200–2208.
12 M. Tiwari and R. Vinu, *J. Anal. Appl. Pyrolysis*, 2025, **189**, 107044.
13 B. A. Oni, O. Oziegbe and O. O. Olawole, *Ann. Agric. Sci.*, 2019, **64**, 222–236.
14 H. Jahangiri, A. Osatiashtiani, M. Ouadi, A. Hornung, A. F. Lee and K. Wilson, *Catalysts*, 2019, **9**, 841.
15 S. Qi, X. Zhang, S. Liu, L. Ran, W. Yi, Z. Li, A. Zhang, D. Zhang and L. Wang, *J. Anal. Appl. Pyrolysis*, 2025, **186**, 106936.
16 S. Kumar, P. Kaur, C.-Y. Hsu, M. Ahmed Mustafa, J. Rani, J. Kaur and S. Kaushal, *Mater. Adv.*, 2025, **6**, 8774–8815.
17 Y. Liu, A. Ali Siyal, C. Zhou, C. Liu, J. Fu, Y. Zhang, B. Yao, L. Chao, H. Yun, J. Dai and X. Bi, *Chem. Eng. J.*, 2024, **485**, 150032.

18 B. Qiu, Y. Wang, D. Zhang and H. Chu, *Chem. Eng. J.*, 2024, **498**, 155362.
19 A. A. Adeleke, P. P. Ikubanni, T. A. Orhadahwe, C. T. Christopher, J. M. Akano, O. O. Agboola, S. O. Adegoke, A. O. Balogun and R. A. Ibikunle, *Heliyon*, 2021, **7**, e08025.
20 B. R. Albuquerque, S. A. 8. Heleno, M. B. P. P. Oliveira, L. Barros and I. C. F. R. Ferreira, *Food Funct.*, 2021, **12**, 14–29.
21 D. Mallick, M. K. Poddar, P. Mahanta and V. S. Moholkar, *Bioresour. Technol.*, 2018, **261**, 294–305.
22 A. Lyons Ceron, R. Ochieng, S. Sarker, O. Järvik and A. Konist, *Energies*, 2024, **17**, 1055.
23 H. H. Muigai, B. J. Choudhury, P. Kalita and V. S. Moholkar, , 2020, **143**, 105839.
24 H. Stančin, M. Šafář, J. Růžičková, H. Mikulčić, H. Raclavská, X. Wang and N. Duić, *Process Saf. Environ. Prot.*, 2021, **145**, 1–11.
25 X. Lin, X. Chen, P. Fu, B. Tang and D. Bi, *Chem. Eng. J.*, 2023, **474**, 145783.
26 Md. E. Hoque, F. Rashid, Md. E. Hoque and F. Rashid, in *Gasification*, 2021, pp. 1–18.
27 A. Trubetskaya, L. von Berg, R. Johnson, S. Moore, J. J. Leahy, Y. Han, H. Lange and A. Anca-Couce, *J. Anal. Appl. Pyrolysis*, 2023, **169**, 105841.
28 H. Nam, S. C. Capareda, N. Ashwath and J. Kongkasawan, *Energy*, 2015, **93**, 2384–2394.
29 J. Giuntoli, W. De Jong, A. H. M. Verkooijen, P. Piotrowska, M. Zevenhoven and M. Hupa, *Energy Fuels*, 2010, **24**, 5309–5319.
30 O. Karlström, A. Brink and M. Hupa, *Fuel*, 2013, **103**, 524–532.
31 A. Aho, N. DeMartini, A. Pranovich, J. Krogell, N. Kumar, K. Eränen, B. Holmbom, T. Salmi, M. Hupa and D. Y. Murzin, *Bioresour. Technol.*, 2013, **128**, 22–29.
32 A. Aho, N. Kumar, A. V. Lashkul, K. Eränen, M. Ziolek, P. Decyk, T. Salmi, B. Holmbom, M. Hupa and D. Y. Murzin, *Fuel*, 2010, **89**, 1992–2000.
33 E. Pienihäkkinen, C. Lindfors, T. Ohra-Aho and A. Oasmaa, *Energy Fuels*, 2022, **36**, 3654–3664.
34 P. Giudicianni, V. Gargiulo, C. M. Grottola, M. Alfè, A. I. Ferreiro, M. A. A. Mendes, M. Fagnano and R. Ragucci, *Energy Fuels*, 2021, **35**, 5407–5478.
35 H. Yang, R. Yan, H. Chen, C. Zheng, D. H. Lee and D. T. Liang, *Energy Fuels*, 2006, **20**, 388–393.
36 P. Francis Prashanth, M. Midhun Kumar and R. Vinu, *Bioresour. Technol.*, 2020, **310**, 123394.
37 M. Tiwari, M. V. P. Babu and R. Vinu, *Chem. Eng. Trans.*, 2024, **109**, 253–258.
38 C. Y. Yang, X. S. Lu, W. G. Lin, X. M. Yang and J. Z. Yao, *Chem. Res. Chin. Univ.*, 2006, **22**, 524–532.
39 C. Grover and B. Choudhury, *Biocatal. Agric. Biotechnol.*, 2024, **57**, 103062.
40 W. Cai, Q. Liu, D. Shen and J. Wang, *J. Anal. Appl. Pyrolysis*, 2019, **138**, 62–69.
41 A. Chotirattanachote, J. Ratthiwal, C. Samart, U. Rashid, N. Hinchiranan, C. Ngamcharussrivichai and J. Ahmad, *Biomass and Bioenergy*, 2026, **206**, 108598.
42 A. E. Pütün, E. Apaydm and E. Pütün, *Energy*, 2004, **29**, 2171–2180.
43 M. Auta, L. M. Ern and B. H. Hameed, *J. Anal. Appl. Pyrolysis*, 2014, **107**, 67–72.
44 N. Abdullah, H. Gerhauser and F. Sulaiman, *Fuel*, 2010, **89**, 2166–2169.
45 Z. Liu, L. Wang, Y. Li and Z. Li, in *International Conference on Advances in Energy, Environment and Chemical Science*, 2016, pp. 221–230.
46 F. Han, M. Wang, X. Ma, L. Yin, D. Chen, Z. Liu and R. Zhang, *Heliyon*, 2023, **9**, e21255.
47 A. Soria-Verdugo, E. Cano-Pleite, A. Passalacqua and R. O. Fox, *Fuel*, 2023, **339**, 127365.
48 M. F. Crowley, R. Seiser, M. A. S. Posada, J. C. Maya, F. Chejne, H. Sitaraman, F. Usseglio-Viretta, A. K. Starace and P. N. Ciesielski, *Energy Fuels*, 2025, **40**, 3136–3158.

